

MAPK-activated transcription factor PxJun suppresses PxABCB1 expression and confers resistance to *Bacillus thuringiensis* Cry1Ac toxin in *Plutella xylostella* (L.)

Article (Accepted Version)

Qin, Jianying, Guo, Le, Ye, Fan, Kang, Shi, Sun, Dan, Zhu, Lihong, Bai, Yang, Cheng, Zhouqiang, Xu, Linzheng, Ouyang, Chunzheng, Xiao, Lifeng, Wang, Shaoli, Wu, Qingjun, Zhou, Xuguo, Crickmore, Neil et al. (2021) MAPK-activated transcription factor PxJun suppresses PxABCB1 expression and confers resistance to *Bacillus thuringiensis* Cry1Ac toxin in *Plutella xylostella* (L.). *Applied and Environmental Microbiology*. ISSN 0099-2240

This version is available from Sussex Research Online: <http://sro.sussex.ac.uk/id/eprint/98922/>

This document is made available in accordance with publisher policies and may differ from the published version or from the version of record. If you wish to cite this item you are advised to consult the publisher's version. Please see the URL above for details on accessing the published version.

Copyright and reuse:

Sussex Research Online is a digital repository of the research output of the University.

Copyright and all moral rights to the version of the paper presented here belong to the individual author(s) and/or other copyright owners. To the extent reasonable and practicable, the material made available in SRO has been checked for eligibility before being made available.

Copies of full text items generally can be reproduced, displayed or performed and given to third parties in any format or medium for personal research or study, educational, or not-for-profit purposes without prior permission or charge, provided that the authors, title and full bibliographic details are credited, a hyperlink and/or URL is given for the original metadata page and the content is not changed in any way.

1 For consideration by:

2 **Applied and Environmental Microbiology**

3 -----

4 **MAPK-activated transcription factor PxJun suppresses *PxABCBI***
5 **expression and confers resistance to *Bacillus thuringiensis* Cry1Ac**
6 **toxin in *Plutella xylostella* (L.)**

7

8 **Running head:** PxJun regulates Cry1Ac resistance in *P. xylostella*

9

10 Jianying Qin^{1,2†}, Le Guo^{2†}, Fan Ye², Shi Kang², Dan Sun², Liuhong Zhu², Yang Bai²,
11 Zhouqiang Cheng², Linzheng Xu², Chunzheng Ouyang², Lifeng Xiao², Shaoli Wang²,
12 Qingjun Wu², Xuguo Zhou³, Neil Crickmore⁴, Xiaomao Zhou^{1*}, Zhaojiang Guo^{2*},
13 Youjun Zhang^{2*}

14 ¹Longping Branch, Graduate School of Hunan University, Changsha 410125, China

15 ²Department of Plant Protection, Institute of Vegetables and Flowers, Chinese
16 Academy of Agricultural Sciences, Beijing 100081, China

17 ³Department of Entomology, University of Kentucky, Lexington, KY 40546-0091, USA

18 ⁴School of Life Sciences, University of Sussex, Brighton, BN1 9QG, UK

19 -----

20 *For correspondence. E-mail: zhouxm1972@126.com (X. Zhou),
21 guozhaojiang@caas.cn (Z. Guo) or zhangyoujun@caas.cn (Y. Zhang).

22 [†]Both authors contributed equally to this work.

Abstract

Deciphering the molecular mechanisms underlying insect resistance to Cry toxins produced by *Bacillus thuringiensis* (Bt) is pivotal for the sustainable utilization of Bt biopesticides and transgenic Bt crops. Previously, we identified that MAPK-mediated reduced expression of the *PxABCB1* gene is associated with Bt Cry1Ac resistance in the diamondback moth, *Plutella xylostella* (L.). However, the underlying transcriptional regulation mechanism remains enigmatic. Herein, the *PxABCB1* promoter in Cry1Ac-susceptible and Cry1Ac-resistant *P. xylostella* strains was cloned and analyzed and found to contain a putative Jun binding site (JBS). A dual-luciferase reporter assay and yeast one-hybrid assay (Y1H) demonstrated that the transcription factor PxJun repressed *PxABCB1* expression by interacting with this JBS. The expression levels of *PxJun* were increased in the midguts of all resistant strains compared to the susceptible strain. Silencing of *PxJun* expression significantly elevated *PxABCB1* expression and Cry1Ac susceptibility in the resistant NIL-R strain, and silencing of *PxMAP4K4* expression decreased *PxJun* expression and also increased *PxABCB1* expression. These results indicate that MAPK-activated PxJun suppresses *PxABCB1* expression to confer Cry1Ac resistance in *P. xylostella*, deepening our understanding of the transcriptional regulation of midgut Cry receptor genes and the molecular basis of insect resistance to Bt Cry toxins.

Importance

The transcriptional regulation mechanisms underlying reduced expression of Bt toxin receptor genes in Bt-resistant insects remain elusive. This study unveils that a

46 transcription factor PxJun activated by the MAPK signaling pathway represses
47 *PxABCB1* expression and confers Cry1Ac resistance in *P. xylostella*. Our results
48 provide new insights into the transcriptional regulation mechanisms of midgut Cry
49 receptor genes and deepen our understanding of the molecular basis of insect
50 resistance to Bt Cry toxins. To our knowledge, this study identified the first
51 transcription factor that can be involved in the transcriptional regulation mechanisms
52 of midgut Cry receptor genes in Bt-resistant insects.

53

54 **Keywords:** *Bacillus thuringiensis*; *Plutella xylostella*; Transcription factor; Jun;
55 ABCB1; Cry1Ac resistance

56 **Introduction**

57 The diverse insecticidal crystal proteins generated by *Bacillus thuringiensis* (Bt) can
58 specifically kill various lepidopteran, coleopteran and dipteran insect pests without
59 causing harm to non-target organisms or the environment; as such, Bt biopesticides
60 and genetically modified Bt crops have been developed and widely used for pest
61 control (1-3). Unfortunately, different insect pests in the field have developed
62 high-level resistance to Bt sprays or Bt crops due to the resulting strong selection
63 pressure, gravely threatening the sustainable application of Bt products (4, 5).
64 Therefore, understanding the molecular mechanisms underlying insect resistance to Bt
65 Cry toxins is crucial for the long-term utilization of these valuable Bt biotechnologies
66 (6, 7).

67 As currently understood, the mode of action of Bt Cry toxins involves multiple
68 steps that occur in the larval midgut, and the binding of Bt Cry toxins to functional
69 receptors in the midgut is a key step in this complex toxicity process (8-10). The
70 identified midgut receptors of Bt Cry toxins include cadherin (CAD), alkaline
71 phosphatase (ALP), aminopeptidase N (APN) and ATP-binding cassette
72 (ABC) transporters (i.e., ABCAs, ABCBs, ABCCs, ABCGs) (11, 12). The
73 down-regulation of midgut Cry receptor genes to reduce toxin-receptor interactions is
74 one of the principal drivers of Bt resistance evolution in diverse insects (13, 14).
75 However, little is known about the transcription regulation mechanisms of these
76 midgut Cry receptor genes.

77 ABCB1, also known as P-glycoprotein (PGP) or MDR1, is one of the
78 best-studied ABC transporters. ABCB1 can serve as a pump to efflux toxic
79 xenobiotics out of cells using ATP-driven energy, and up-regulation of the *ABCB1*
80 gene has been reported to be involved in multidrug resistance (MDR) in mammals (15)
81 and resistance to chemical and biological pesticides in insects (16-19). Moreover,
82 studies in recent years have found that ABCB1 can also serve as a functional midgut
83 receptor of Bt Cry3 toxins, and its gene mutation is associated with high-level
84 resistance to Bt Cry3 toxins in *Diabrotica virgifera virgifera* and *Chrysomela tremula*
85 (20-22). Meanwhile, we found that down-regulation of *ABCB1* is directly associated
86 with Cry1Ac resistance in *P. xylostella* (23, 24). Although research on the
87 transcriptional regulatory mechanisms of *ABCB1* expression has made great progress
88 in mammals (25, 26), little is known about this phenomenon in insects.

89 Recently, our studies have shown that the insect hormone-activated
90 mitogen-activated protein kinase (MAPK) signaling pathway can act as a common
91 switch to *trans*-regulate the differential expression of multiple midgut genes,
92 including ALP, APNs (*APN1*, *APN3a*, *APN5* and *APN6*) and ABC transporters
93 (*ABCB1*, *ABCC1*, *ABCC2*, *ABCC3* and *ABCG1*), thereby conferring Bt Cry1Ac
94 resistance in *P. xylostella* without fitness costs (14, 23, 24, 27, 28). The above
95 researches have also indicated that there is a significant level of redundancy in
96 receptors such that multiple proteins within a given insect can act as functional
97 receptors and that change of individual gene results in incremental increase in
98 resistance. The involvement of the MAPK cascades indicating that there are some

99 MAPK-responsive downstream transcription factors (TFs) that regulate the expression
100 of these midgut genes, including *ABCB1* (29). Moreover, some studies have also
101 found that TFs such as FOXA and GATAe can positively regulate the expression of
102 some Bt Cry1Ac receptor genes, including *ABCC2*, *ABCC3*, *ALP* and *CAD*, in
103 different insect cell lines (30, 31). Indeed, we have identified a MAPK-activated
104 transcription factor *CREB* that can increase the expression of a P450 gene *CYP6CM1*
105 thereby leading to imidacloprid resistance in *Bemisia tabaci* (32). Nonetheless, the
106 TFs that regulate the reduction in expression of midgut receptor genes, including
107 *ABCB1*, in insect resistance to Bt Cry toxins remain largely unknown.

108 Here, our work has shown that a TF called PxJun can directly bind to the
109 promoter region of *PxABCB1* to reduce its expression. Furthermore, midgut *PxJun*
110 expression was significantly higher in all the Cry1Ac-resistant strains than in the
111 Cry1Ac-susceptible strain. Silencing of *PxJun* expression up-regulated *PxABCB1*
112 transcription and enhanced larval susceptibility to Cry1Ac toxin in the
113 Cry1Ac-resistant NIL-R strain, and silencing of *PxMAP4K4* expression inhibited
114 *PxJun* and increased *PxABCB1* transcription. These results indicate that PxJun
115 activated by the MAPK signaling pathway participates in Cry1Ac resistance in *P.*
116 *xylostella* by inhibiting the expression of the *PxABCB1* gene. Our results provide
117 important insights into the transcriptional regulation of Bt toxin receptors, providing a
118 better understanding of the evolution of insect resistance to Bt Cry toxins.

119 Results

120 *PxABCBI* promoter analyses in susceptible and resistant strains

121 Having previously observed that differential expression of *PxABCBI* associates with
122 resistance to the Bt Cry1Ac toxin in *P. xylostella* (23, 24), we sought to compare the
123 promoter region of this gene between a susceptible and resistant strain in order to
124 investigate possible reasons for this differential expression.

125 We amplified the 5'-flanking region of the *PxABCBI* gene from gDNA samples
126 of the Cry1Ac-susceptible strain DBM1Ac-S and its near-isogenic Cry1Ac-resistant
127 strain NIL-R. Analysis of the *PxABCBI* promoter sequence revealed a conserved
128 initiator of transcription site (Inr) motif 5'-TCAGT-3' located 127 nucleotides (nt)
129 upstream of the start codon (ATG) of the *PxABCBI* gene. The adenine (A) of the Inr
130 was designed as the transcriptional start site (TSS) and marked as "+1" (Fig. S1).
131 With respect to promoter identification no typical TATA box was found near the
132 TSS, although a putative CAAT box was predicted 139 nt upstream of the TSS (Fig.
133 S1). Nucleotide sequence alignment showed that multiple single nucleotide
134 polymorphism (SNP) sites existed in the *PxABCBI* promoters of the two strains and
135 that the *PxABCBI* promoter in the NIL-R strain contained a number of deletions as
136 well as a small insertion compared with that in the DBM1Ac-S strain (Fig. 1A and
137 Fig. S1).

138 To investigate whether the differences in the 5'-flanking region sequences
139 between DBM1Ac-S and NIL-R strains lead to differences in promoter activity, and
140 thus cause differential expression of the *PxABCBI* gene, a transcriptional reporter

141 assay was employed. Three full-length and truncated promoters to reflect regions of
142 similarity and dissimilarity between the two strains were cloned into the pGL4.10
143 vector to drive the expression of the luciferase reporter gene (Fig. 1). The relative
144 luciferase activities of these *PxABCBI* promoter recombinant plasmids were
145 detected in S2 cells at 48 h post-transfection. The results indicated that there was no
146 significant difference in activity for any of the *PxABCBI* promoter regions (Fig. 1B),
147 suggesting that genomic differences were not responsible for the altered expression
148 of *PxABCBI* in the resistant strain. What was noticeable however was that the
149 promoter activity was significantly reduced when the section between -280 and +125
150 was used, despite this containing the putative CAAT box promoter motif (Fig. 1B
151 and Fig.S1).

152

153 **Identification of the critical regulatory regions in the *PxABCBI* promoter**

154 To investigate the loss of promoter activity associated with the -280/+125 region, we
155 created a further range of constructs containing decreasing amounts of the promoter
156 region from the DBM1Ac-S strain (Fig. 2). The data from these constructs
157 confirmed that promoter activity was reduced once sequences upstream of -460 were
158 removed. Interestingly though, the promoter activity was partially restored when the
159 deletion extended as far as -72 (Fig. 2). Based on the luciferase activity data, these
160 two important regulatory regions in *PxABCBI* promoter from -621 to -460, and from
161 -112 to -72 likely contain critical positive and negative regulatory elements,
162 respectively, suggesting that they could potentially control *PxABCBI* expression

163 through a combination of *cis*-regulatory elements and *trans*-acting factors (33).

164

165 **The transcription factor PxJun represses *PxABCB1* promoter activity**

166 Informatic analyses were undertaken to identify putative transcription factor (TF)
167 binding sites. Potential sites for CncC, Vvl and Ubx were predicted in the positive
168 regulatory region and the binding sites of Jun and Ubx were predicted in the core
169 negative regulatory region (Fig. 3A and Fig. S1). To explore whether these proteins
170 were involved in the transcriptional regulation of the *PxABCB1* gene, the full-length
171 coding region of each TF was cloned by PCR amplification and subcloned into the
172 expression vector pAc5.1. They were then co-transfected into S2 cells along with the
173 luciferase reporter plasmid bearing the full *PxABCB1* promoter region. The
174 co-transfection assays revealed that PxJun significantly decreased the activity of the
175 *PxABCB1* promoter compared with the control, while other TFs had little effect on
176 promoter activity (Fig. 3B), suggesting that PxJun might be involved in the negative
177 regulation of *PxABCB1* expression through interacting with the Jun binding site
178 (JBS).

179

180 **PxJun interacts with the JBS to repress *PxABCB1* promoter activity**

181 To confirm that PxJun inhibits promoter activity through the predicted JBS between
182 -112 and -72 (Fig. 3A), recombinant plasmids bearing *PxABCB1* promoters
183 containing a JBS deletion or mutation were constructed and co-transfected with the
184 PxJun plasmid into S2 cells. The luciferase activity of the *PxABCB1* promoter

185 containing normal JBS was significantly decreased by PxJun, whereas the activities
186 of the JBS deleted or mutated promoters showed no change compared with the
187 control (Fig. 4A). These results suggested that PxJun repressed *PxABCB1* promoter
188 activity mainly through the identified JBS. Subsequently, a yeast one-hybrid (Y1H)
189 assay was carried out to further test the interaction between PxJun and the JBS. The
190 yeast strain containing the PxJun prey vector and normal JBS bait grew normally on
191 SD/-Leu medium supplemented with 500 ng/mL AbA, while the yeast strain
192 containing the PxJun prey vector and mutant JBS-M bait did not grow (Fig. 4B).
193 This result indicated that the PxJun prey plasmid interacted with the JBS but not the
194 JBS-M bait. Together, the above results confirmed that PxJun suppressed the
195 promoter activity of the *PxABCB1* gene by interacting with the JBS.

196

197 **Analysis of the PxJun protein and its possible interaction with PxFos**

198 The PxJun protein contains two characteristic domains: the Jun domain at the
199 N-terminus and the bZIP_Jun domain at the C-terminus (Fig. S2). The bZIP_Jun
200 domain consists of a basic DNA-binding domain (DBD) for specific DNA
201 recognition and binding, followed by a leucine zipper domain for protein
202 dimerization (Fig. S3) (29). Both domains are conserved among different insects and
203 mammals (Fig. S2 and Fig. S3). We performed a phylogenetic analysis of PxJun to
204 determine the evolutionary relationships among c-Jun proteins in different species
205 (Fig. S2). The results showed that the c-Jun proteins are evolutionarily conserved
206 and clearly clustered into groups corresponding to each insect order; as expected, the

207 mammalian c-Jun proteins also grouped into one cluster (Fig. S2).

208 Jun-related subfamily members typically interact with themselves or other
209 proteins, and function as dimers in their regulatory role, and Fos subfamily proteins
210 are the most common co-factors (34, 35). Thus, we aimed to further explore whether
211 the PxFos protein is also involved in the regulation of *PxABCB1* transcription with
212 PxJun. A recombinant plasmid encoding PxFos with or without PxJun was
213 co-transfected with the *PxABCB1* promoter into S2 cells to measure the activity of
214 the luciferase reporter. Transfection of PxFos alone or in combination with PxJun
215 had no significant effect on the activity of the *PxABCB1* promoter (Fig. 5),
216 indicating that the PxFos protein did not participate in the regulation of the
217 *PxABCB1* gene.

218

219 **Increased expression levels of the *PxJun* gene in resistant strains**

220 The spatio-temporal transcription profiles of the *PxJun* gene were monitored by
221 qPCR in different tissues of fourth-instar DBM1Ac-S larvae and different
222 developmental stages. The tissue expression profile showed that the *PxJun* gene was
223 widely expressed in different tissues with no obvious tissue-specific expression
224 pattern, implying that the *PxJun* gene plays important roles in a variety of tissues
225 (Fig. S4). Meanwhile, developmental expression analysis indicated that the *PxJun*
226 gene was also expressed in different periods with no obvious stage-specific
227 expression pattern (Fig. S4), suggesting that the *PxJun* gene is involved in the
228 regulation of growth, development and reproduction in *P. xylostella*.

229 To further investigate the relationship between *PxJun* and *PxABCB1*, the
230 transcript levels of *PxJun* were detected in the midgut tissues of fourth-instar larvae
231 of different *P. xylostella* strains. As indicated by the qPCR results, the expression
232 levels of the *PxJun* gene were significantly higher in all four Cry1Ac-resistant
233 strains than in the susceptible DBM1Ac-S strain (Fig. 6). The expression trend of
234 *PxJun* was negatively correlated with the *PxABCB1* expression trend in the midgut
235 tissues of different strains (detected in our previous study) (23), whereas it was
236 positively correlated with Cry1Ac resistance level, supporting the concept that *PxJun*
237 promotes Cry1Ac resistance by repressing *PxABCB1* expression.

238

239 **Silencing *PxJun* enhances *PxABCB1* expression and susceptibility to Cry1Ac** 240 **toxin**

241 To validate whether *PxJun* depresses *PxABCB1* expression in *P. xylostella*,
242 *PxJun*-specific dsRNA was synthesized and injected into third-instar NIL-R larvae.
243 The transcription levels of *PxJun* and *PxABCB1* were measured by qPCR after 48 h.
244 The expression of *PxJun* was reduced by approximately 50% in the midguts of
245 dsRNA-injected larvae compared with controls; by contrast, the transcriptional level
246 of *PxABCB1* in their midguts was significantly increased compared to that of
247 controls (Fig. 7A). In addition, toxicity bioassays with 1000 mg/L Cry1Ac protoxin
248 were carried out at 48 h post-injection. The mortality of the *PxJun*-silenced larvae
249 was dramatically increased (from 10% to 35.56%) (Fig. 7B). These data again
250 supported the role of *PxJun* in negatively controlling the expression of *PxABCB1* in

251 *vivo*, contributing to Cry1Ac resistance in *P. xylostella*.

252

253 **The MAPK signaling pathway activates *PxJun* transcription**

254 Jun subfamily proteins are typical downstream targets of the MAPK signaling
255 pathway and can be activated at the transcriptional and protein phosphorylation
256 levels in mammals (34, 36, 37). Our previous studies revealed that the insect
257 hormone-activated MAPK signaling pathway regulates the reduced expression of
258 multiple midgut receptors including *PxABCB1* gene in resistant *P. xylostella* strains
259 (24). Thus, we speculated that the decrease in *PxABCB1* expression might be
260 controlled by MAPK-responsive *PxJun*. To investigate whether *PxJun* expression
261 leading to the down-regulation of *PxABCB1* is induced by the MAPK signaling
262 pathway, we silenced *PxMAP4K4* expression in resistant NIL-R larvae and then
263 detected the expression levels of *PxJun* and *PxABCB1* at different periods (Fig. 8).
264 The results reflected that after *PxMAP4K4* dsRNA injection, the transcript level of
265 *PxJun* decreased, while the expression level of *PxABCB1* increased (Fig.
266 8). Therefore, *PxJun* responded to MAPK signaling pathway and repressed the
267 expression of the *PxABCB1* gene in Cry1Ac-resistant *P. xylostella*.

268 Discussion

269 Down-regulation of Bt Cry toxin receptor genes in the midgut usually results in
270 high-level Bt resistance in insects; nevertheless, the specific transcriptional
271 regulation mechanisms of these midgut genes remain poorly understood. Changes in
272 gene expression can result from changes in *trans*-regulatory factors and
273 *cis*-regulatory elements (TFBS in promoter, enhancer and silencer) (38). In this study,
274 we revealed that the MAPK-activated TF PxJun regulates the reduced expression of
275 the *PxABCB1* gene, thereby mediating Bt Cry1Ac resistance in *P. xylostella*.

276 Jun subfamily members in mammals include c-Jun, JunB and JunD, important
277 stress-responsive TFs that are activated by the MAPK signaling pathway under
278 various physiological and external stimuli and participate in multiple cellular
279 processes, such as cell proliferation, differentiation, apoptosis and inflammation (34,
280 39). Intriguingly, whereas there are three Jun paralogs in mammals, only one Jun
281 protein, a homolog of the mammalian c-Jun, has been identified in insects (36, 40).
282 As in mammals, the MAPK signaling pathway in *D. melanogaster* can activate DJun
283 in response to various stimuli to ensure normal development, immunity and
284 homeostasis (37, 41).

285 Jun-related subfamily members belong to the basic leucine zipper (bZIP) family
286 of proteins, which typically exert their functions through homodimerization or
287 heterodimerization to form an AP-1 complex (34, 35). Jun proteins in animals
288 participate in essential biological processes, including cell proliferation,
289 differentiation, apoptosis and immune response (39). *PxJun* is a homolog of

290 mammalian *c-Jun*. We demonstrated that PxJun can specifically bind to the JBS and
291 inhibit the promoter activity of the *PxABCB1* gene. In mammals, activated c-Jun can
292 act as an activator or repressor to control *MDR1* (*ABCB1*) expression in different
293 cancer cells (25, 42-45). Therefore, c-Jun appears to play a dual regulatory role in
294 the regulation of *ABCB1* expression in different types of cells and species, probably
295 depending on its binding partners and on the cellular environment.

296 In mammals, the AP-1 complexes Jun-Jun and Jun-Fos preferentially bind to
297 12-*O*-tetradecanoylphorbol-13-acetate (TPA) response elements (TRE,
298 5'-TGA(C/G)TCA-3'), while Jun-ATF preferentially binds to the cAMP response
299 element (CRE, 5'-TGACGTCA-3') (35, 39). Distinct cofactors of Jun have different
300 effects on the DNA binding affinity and function of the dimer, thus greatly
301 expanding the spectrum of regulated genes (34). Our structural analysis of the PxJun
302 protein showed a highly conserved bZIP_Jun domain for DNA binding and protein
303 interaction at the C-terminus. Fos is the most common partner of Jun (34, 35).
304 However, we demonstrated that the PxFos protein did not participate in the
305 regulation of the *PxABCB1* gene. Thus, further study is needed to identify whether
306 additional TFs interact with PxJun to co-regulate *PxABCB1* expression in the midgut,
307 which will help us understand the complex functions of AP-1.

308 Mammalian AP-1 family members are expressed in a cell- and stage-dependent
309 manner during development and under different stimuli, thereby mediating different
310 transcriptional levels of specific target genes (34). In *D. melanogaster*, *DJun*
311 expression is observed in all tissues and developmental stages (46). Similarly, we

312 found that the *PxJun* gene is extensively expressed in multiple tissues and
313 developmental stages of *P. xylostella*. The temporally and spatially broad expression
314 pattern of c-Jun implies its essential role in maintaining immunity and homeostasis,
315 normal growth and development, and response to various stress factors (35, 39, 47).

316 Jun subfamily proteins in mammals are activated both at the transcriptional
317 level and via post-translational modification by the MAPK signaling pathway in
318 response to many physiological and environmental stimuli, affecting the
319 transactivation potential, DNA binding capacity and stability of AP-1 components
320 (34, 36, 37). Studies in human cells found that c-Jun can be activated by the MAPK
321 signaling pathway, leading to elevated transcript and phosphorylation levels and thus
322 regulating the expression of the *MDR1* (*ABCB1*) gene (43, 44, 48, 49). Silencing of
323 *PxMAP4K4* expression down-regulated *PxJun* and up-regulated *PxABCB1*,
324 demonstrating that the expression of the *PxABCB1* gene is negatively regulated by
325 the MAPK-responsive *PxJun* in *P. xylostella*. Persistent alteration of AP-1 activity
326 and/or *ABCB1* expression can induce the oncogenic transformation of cells and
327 tumor formation, as well as the development of chemo-resistance in mammals (39).
328 In fact, the expression trend of *PxJun* in midgut tissues of different *P. xylostella*
329 strains is similar to that of *PxMAP4K4* and opposite to that of *PxABCB1* (23, 24, 27).
330 Thus, a model explaining the transcriptional regulation mechanisms of reduced
331 expression of the *PxABCB1* gene is shown in Fig. 9. In the Bt-resistant *P. xylostella*
332 larvae, the activated MAPK signaling pathway can induce *PxJun* transcription
333 thereby leading to reduction of *PxABCB1* gene expression and causing Cry1Ac

334 resistance. Therefore, the MAPK/c-Jun signaling cascade might be a common
335 mechanism of transcriptional regulation of the *ABCB1* gene. Since the MAPK
336 pathway has been shown to regulate the expression of a number of Cry1Ac receptors
337 within *P. xylostella*, it is possible that PxJun is directly involved in the
338 downregulation of other receptors and therefore that the increase in mortality
339 observed in Fig. 7B may not be solely attributed to *PxABCB1* overexpression.
340 Further research is needed to evaluate whether the MAPK signaling pathway
341 activates PxJun at both the transcript and phosphorylation levels, and whether PxJun
342 also participates in the regulation of other receptors.

343 In conclusion, we found that PxJun negatively regulates *PxABCB1* expression
344 by interacting with the JBS in the *PxABCB1* promoter, and the activated MAPK
345 cascade enhances *PxJun* expression and thus represses *PxABCB1* expression to
346 result in Cry1Ac resistance in *P. xylostella*. This study provides new insights into the
347 transcriptional regulation mechanisms of midgut receptor genes and lays the
348 foundation for comprehensively understanding the complex molecular mechanisms
349 of insect resistance to Bt Cry toxins.

350 **Material and methods**

351 **Insect strains and cell line**

352 The five *P. xylostella* strains used in this study, including one Bt-susceptible and four
353 Bt-resistant strains, were described previously (27, 50, 51). In brief, the DBM1Ac-S
354 strain has been maintained in the laboratory without exposure to any Bt
355 products/toxins or any other insecticides. The four Bt-resistant strains, DBM1Ac-R,
356 NIL-R, SZ-R and SH-R exhibit different levels of resistance to Bt Cry1Ac protoxin
357 or Bt *var. kurstaki* (Btk) formulation. Their resistance ratios are approximately 3500,
358 4000, 450, and 1900 folds that of the susceptible DBM1Ac-S strain, respectively.
359 The larvae of all strains were reared on Jing Feng No. 1 cabbage (*Brassica oleracea*
360 *var. capitata*) at 25 °C, 65% relative humidity (RH) and a 16:8 (light:dark)
361 photoperiod. Adults were supplied with a 10% honey/water solution.

362 The *Drosophila melanogaster* S2 cell line was transfected for the
363 dual-luciferase reporter assay. S2 cells were cultured in HyClone SFX-insect
364 medium (Thermo Fisher Scientific, Waltham, MA, USA) supplemented with
365 penicillin-streptomycin (Gibco, Rockville, MD, USA) at 27 °C.

366

367 **Toxin preparation and toxicity bioassay**

368 The Cry1Ac protoxin preparation and subsequent leaf-dip bioassay were performed
369 as described previously (52). Briefly, the Cry1Ac protoxin was isolated and purified
370 from Btk strain HD-73, and its protein concentration was quantified and stored in 50
371 mM Na₂CO₃ (pH 9.6) for subsequent toxicity bioassays. A three-day leaf-dip

372 bioassay was conducted using third-instar *P. xylostella* larvae. Ten individuals in
373 each group were used, and the bioassays were repeated four times for each Cry1Ac
374 concentration. The larval mortality of the control did not exceed 5%.

375

376 **gDNA extraction, promoter cloning and TFBS prediction**

377 Genomic DNA (gDNA) was isolated from fourth-instar *P. xylostella* larvae using the
378 TIANamp Genomic DNA Kit (Tiangen, Beijing, China) following the
379 manufacturer's instructions. A pair of specific PCR primers to amplify the *PxABCB1*
380 promoter was designed based on the 5'-flanking sequence of the *PxABCB1* gene in
381 the *P. xylostella* genome dataset of LepBase
382 (http://ensembl.lepbase.org/Plutella_xylostella_pacbio1/Info/Index). PrimeSTAR
383 Max DNA Polymerase (TaKaRa, Dalian, China) was used according to the
384 manufacturer's protocol for all PCR amplifications in this study. The PCR products
385 were subsequently purified and ligated into pEASY-T1 vectors (TransGen, Beijing,
386 China) for sequencing. Transcription factor binding sites (TFBSs) in the *PxABCB1*
387 promoter region were *in silico* predicted via the JASPAR
388 database (<http://jaspar.genereg.net>) and PROMO virtual laboratory
389 (http://alggen.lsi.upc.es/cgi-bin/promo_v3/promo/promoinit.cgi?dirDB=TF_8.3).

390

391 **Sample preparation, RNA isolation and cDNA synthesis**

392 Samples at different developmental stages (eggs, first- to fourth-instar larvae,
393 prepupae, pupae, 1-day-old virgin male and female adults) were collected from the

394 susceptible DBM1Ac-S strain, and five tissues (head, midgut, Malpighian tubules,
395 integument and testis) were dissected from fourth-instar *P. xylostella* larvae in
396 ice-cold insect Ringer's solution (130 mM NaCl, 0.5 mM KCl, 0.1 mM CaCl₂).

397 Total RNA from different samples was extracted with TRIzol reagent
398 (Invitrogen, Carlsbad, CA, USA) following the manufacturer's instructions. The
399 first-strand cDNA used for subsequent gene cloning was synthesized using the
400 PrimeScript II First Strand cDNA Synthesis Kit (TaKaRa, Dalian, China) according
401 to the manufacturer's protocol.

403 **TF cloning and sequence analysis**

404 The initial open reading frames (ORFs) of *Jun*, *Fos*, *cap 'n' isoform C* (*CncC*) and
405 *ultrabithorax* (*Ubx*) genes in *P. xylostella* were retrieved from the GenBank database
406 (<https://www.ncbi.nlm.nih.gov/>) under accession numbers XM_011559543,
407 XM_011549928, XM_011570739 and KP245729, respectively. In addition, the ORF
408 of the *ventral veins lacking* (*Vvl*) gene in *P. xylostella* was obtained from the
409 LepBase (<http://ensembl.lepbase.org/>, Gene ID: g11291). All the ORFs of these
410 genes were further corrected *in silico* with the assistance of our previous *P.*
411 *xylostella* midgut transcriptome database (53). Using specific primers for PCR
412 amplification (Table S1), the full-length coding sequences (CDSs) of PxJun
413 (GenBank accession no. MW446637) and four other genes were cloned, and each
414 obtained CDS was translated into amino acid sequences using the ExPASy translate
415 tool (<https://web.expasy.org/translate/>). The presence of conserved domains in the

416 PxJun protein was analyzed using the Conserved Domain Database (CDD) at NCBI
417 (<https://www.ncbi.nlm.nih.gov/cdd/>). Multiple sequence alignment was conducted
418 using Clustal Omega (<http://www.ebi.ac.uk/Tools/msa/clustalo/>) and was further
419 formatted using GeneDoc 2.7 software (<http://genedoc.software.informer.com/2.7/>).
420

421 **Phylogenetic analysis**

422 The Jun protein sequences used for alignment and phylogenetic analysis in insects
423 and representative mammals were obtained from the GenBank database. A
424 phylogenetic tree was built using MEGA 7.0 software
425 (<https://www.megasoftware.net/>) with the neighbor-joining (NJ) method, “p-distance”
426 model and 1000 bootstrap replicates.
427

428 **Dual-luciferase assay**

429 The 5'-flanking sequence of the *PxABCB1* gene was truncated into a series of
430 fragments of different sizes. All the fragments were subcloned into linearized
431 pGL4.10 vector (double digests with *Bgl*III and *Kpn*I) using the In-Fusion HD
432 Cloning Kit (Clontech, Mountain View, CA, USA). The In-Fusion primers used for
433 promoter amplification are listed in **Table S1**. In addition, full-length promoters with
434 JBS mutation/deletion were obtained by gene synthesis (TsingKe, Beijing, China).
435 The ORFs of TFs were ligated into linearized pAc5.1/V5-His B expression vector
436 (hereinafter referred to as “pAc5.1”, double digested with *Kpn*I and *Xho*I) using the
437 In-Fusion HD Cloning Kit (Clontech, Mountain View, CA, USA). The In-Fusion

438 primers used for TF amplification are listed in Table S2. The pGL4.73 vector
439 (Promega, Madison, WI, USA) containing a *Renilla* luciferase gene was used as an
440 internal control.

441 Vector transfection was performed using Lipofectamine 2000 transfection
442 reagent (Thermo Fisher Scientific, Waltham, MA, USA). S2 cells were seeded at a
443 density of 5×10^5 cells per well in 400 μ L medium without antibiotics in a 24-well
444 plate 6 h before transfection. To detect promoter activity, the pGL4.10-promoter
445 reporter plasmid (600 ng) was co-transfected with pGL4.73 (200 ng), and the empty
446 pGL4.10 vector was used as the control vector. To determine the effect of TF on
447 promoter activity, the pAc5.1-TF expression plasmid (600 ng) and
448 pGL4.10-promoter reporter plasmid (200 ng) were co-transfected with pGL4.73 (100
449 ng), and the empty pAc5.1 plasmid was used as the control vector. For each
450 transfection reaction, the plasmids and transfection reagent were diluted in 100 μ L
451 medium without antibiotics, incubated at room temperature for 15 min and then
452 added to each well. After 48 h of transient transfection, luciferase activity was
453 measured on a GloMax 96 Microplate Luminometer (Promega, Madison, WI, USA)
454 by using the Dual-Luciferase Reporter Assay System (Promega, Madison, WI, USA)
455 according to the manufacturer's protocol. The luciferase activity was calculated by
456 normalizing the firefly luciferase level to the *Renilla* luciferase level. The relative
457 luciferase activity (fold) was calculated by setting the activity of the control to an
458 arbitrary value of 1. Three biological replicates and four technical replicates were
459 conducted for each transfection experiment. The statistical significance of

460 differences between different groups were analyzed by one-way ANOVA with
461 Duncan's test ($p < 0.05$).

462

463 **Yeast one-hybrid (Y1H) assay**

464 A yeast one-hybrid (Y1H) assay was performed using the Matchmaker Gold Yeast
465 One-Hybrid System (Clontech, Mountain View, CA, USA) according to the
466 manufacturer's instructions. Three tandem copies of the predicted JBS
467 (5'-AGAAAGAAATGAGAGATACG-3') or mutant JBS
468 (5'-AGAGGAGGGCAGAGAGCACG-3') were ligated to linearized pAbAi vector
469 (double digested with *XhoI* and *HindIII*) to construct bait plasmids. The bait strains
470 were generated by integrating the pBait-AbAi vector (linearized with *BstBI*) into the
471 Y1HGold yeast genome and then selected on SD/-Ura medium. After 3-5 days at
472 30 °C, colonies were picked and analyzed by colony PCR and sequenced to further
473 identify bait sequence inserts. For each confirmed bait strain, the minimal inhibitory
474 concentration of aureobasidin A (AbA) to suppress basal expression of the bait
475 construct was determined (less than 1000 ng/mL), and this AbA concentration was
476 used to screen the prey-bait interaction. *PxJun* cDNA was subcloned into linearized
477 pGADT7 vector (double digested with *EcoRI* and *XhoI*) to construct a prey plasmid,
478 which was then transformed into the bait strains and selected on SD/-Leu medium
479 with the minimal AbA inhibitory concentration. After 3-5 days at 30 °C, colonies
480 were picked, analyzed by colony PCR and sequenced to confirm the prey protein
481 inserts. The confirmed positive interaction colony was rescreened on SD/-Leu

482 medium with AbA to establish individual interaction strains. The positive control
483 was generated by co-transforming the pGADT7-p53 and pAbAi-p53 plasmids into
484 the Y1HGold strain. A negative control was created by co-transforming the empty
485 pGADT7 with the normal pAbAi-JBS plasmids into the Y1HGold strain.

486

487 **qPCR analysis**

488 As mentioned before (14, 23), the transcript levels of the *PxJun* and *PxABCB1* genes
489 were quantified by real-time quantitative PCR (qPCR) using the specific primers
490 listed in Table S3. The qPCR experiment was run on the QuantStudio 3 Real-Time
491 PCR System (Applied Biosystems, USA) using FastFire qPCR PreMix (SYBR
492 Green) (Tiangen, Beijing, China) according to the manufacturer's instructions. Three
493 biological replicates and four technical replicates were performed for each
494 experiment. The relative expression levels of target genes were determined using the
495 $2^{-\Delta\Delta CT}$ method and normalized to the internal control ribosomal protein *L32* (*RPL32*)
496 gene (GenBank accession no. AB180441). The statistical significance of differences
497 between groups were analyzed by one-way ANOVA with Duncan's test ($p < 0.05$).

498

499 **RNA interference**

500 RNA interference (RNAi) of *PxMAP4K4* and *PxJun* was carried out to investigate
501 the regulatory relationships among the *PxMAP4K4*, *PxJun* and *PxABCB1* genes and
502 to explore whether the *PxJun* gene is involved in Cry1Ac resistance in *P. xylostella*.
503 The cDNA fragments of *PxMAP4K4*, *PxJun* or *EGFP* used as templates for

subsequent dsRNA synthesis were amplified by gene-specific dsRNA primers containing a T7 promoter on the 5' end (Table S3). The gene-specific primer set used to produce dsRNA of *PxJun* was designed for the 5'-terminal gene-specific region and not for the 3'-terminal conserved bZIP_Jun region to avoid potential off-target effects, and we could not detect any specific hits to other Jun genes by BLASTN search of GenBank (<https://www.ncbi.nlm.nih.gov/>) or the *P. xylostella* genome database (LepBase: http://ensembl.lepbase.org/Plutella_xylostella_pacbio1/Info/Index), further confirming the specificity of the selected dsRNA fragment. *PxMAP4K4*, *PxJun* or *EGFP* dsRNA was synthesized using the T7 RiboMAX Express RNAi System (Promega, Madison, WI, USA) as indicated by the manual.

The protocol for RNAi experiments in the early third-instar larvae of the resistant NIL-R strain was conducted by dsRNA microinjection as mentioned earlier (54). Thirty larvae were microinjected with buffer, dsEGFP (300 ng), dsPxJun (300 ng) or dsPxMAP4K4 (300 ng) for each treatment, and three biological repeats were performed. The injected larvae were reared and subjected to qPCR analysis at different times. In addition, toxicity bioassays were carried out at 48 h post-injection. The larvae were fed cabbage containing 1000 mg/L Cry1Ac protoxin (LC₁₀ value for NIL-R larvae) for 72 h to calculate larval mortality as described previously (14, 52). The significance of the differences between the treatment and control groups were determined by one-way ANOVA with Duncan's test ($p < 0.05$).

525

526 **Data availability**

527 The full-length cDNA sequence of the cloned *PxJun* gene in this study has been
528 deposited in the GenBank database under accession number MW446637.

530 **Acknowledgments**

531 This work was supported by the National Natural Science Foundation of China
532 (31630059; 31701813; 32022074), the Beijing Key Laboratory for Pest Control and
533 Sustainable Cultivation of Vegetables and the Science and Technology Innovation
534 Program of the Chinese Academy of Agricultural Sciences
535 (CAAS-ASTIP-IVFCAAS).

537 **Conflict of interest**

538 The authors declare no conflict of interest.

540 **References**

- 541 1. Bravo A, Likitvivatanavong S, Gill SS, Soberón M. 2011. *Bacillus thuringiensis*:
542 A story of a successful bioinsecticide. *Insect Biochem Mol Biol* 41:423–431.
- 543 2. Sanahuja G, Banakar R, Twyman RM, Capell T, Christou P. 2011. *Bacillus*
544 *thuringiensis*: a century of research, development and commercial applications.
545 *Plant Biotechnol J* 9:283–300.
- 546 3. Sanchis V. 2011. From microbial sprays to insect-resistant transgenic plants:
547 history of the biopesticide *Bacillus thuringiensis*. A review. *Agron Sustain Dev*

- 548 31:217–231.
- 549 4. Tabashnik BE, Brévault T, Carrière Y. 2013. Insect resistance to Bt crops: lessons
550 from the first billion acres. *Nat Biotechnol* 31:510–521.
- 551 5. Tabashnik BE, Carrière Y. 2017. Surge in insect resistance to transgenic crops
552 and prospects for sustainability. *Nat Biotechnol* 35:926–935.
- 553 6. Peterson B, Bezuidenhout CC, Van den Berg J. 2017. An overview of
554 mechanisms of Cry toxin resistance in lepidopteran insects. *J Econ Entomol*
555 110:362–377.
- 556 7. Xiao Y, Wu K. 2019. Recent progress on the interaction between insects and
557 *Bacillus thuringiensis* crops. *Phil Trans R Soc B* 374:20180316.
- 558 8. Pardo-López L, Soberón M, Bravo A. 2013. *Bacillus thuringiensis* insecticidal
559 three-domain Cry toxins: mode of action, insect resistance and consequences for
560 crop protection. *FEMS Microbiol Rev* 37:3–22.
- 561 9. Jurat-Fuentes JL, Crickmore N. 2017. Specificity determinants for Cry
562 insecticidal proteins: Insights from their mode of action. *J Invertebr Pathol*
563 142:5–10.
- 564 10. de Bortoli CP, Jurat-Fuentes JL. 2019. Mechanisms of resistance to
565 commercially relevant entomopathogenic bacteria. *Curr Opin Insect Sci* 33:56–
566 62.
- 567 11. Pigott CR, Ellar DJ. 2007. Role of receptors in *Bacillus thuringiensis* crystal
568 toxin activity. *Microbiol Mol Biol Rev* 71:255–281.
- 569 12. Wu C, Chakrabarty S, Jin M, Liu K, Xiao Y. 2019. Insect ATP-binding cassette

- (ABC) transporters: roles in xenobiotic detoxification and Bt insecticidal activity.
Int J Mol Sci 20:2829.
13. Adang MJ, Crickmore N, Jurat-Fuentes JL. 2014. Diversity of *Bacillus thuringiensis* crystal toxins and mechanism of action. Adv Insect Physiol 47:39–87.
14. Guo Z, Kang S, Zhu X, Xia J, Wu Q, Wang S, Xie W, Zhang Y. 2015. Down-regulation of a novel ABC transporter gene (*Pxwhite*) is associated with Cry1Ac resistance in the diamondback moth, *Plutella xylostella* (L.). Insect Biochem Mol Biol 59:30–40.
15. Silva R, Vilas-Boas V, Carmo H, Dinis-Oliveira RJ, Carvalho F, de Lourdes Bastos M, Remiao F. 2015. Modulation of P-glycoprotein efflux pump: induction and activation as a therapeutic strategy. Pharmacol Ther 149:1–123.
16. Lanning CL, Ayad HM, Abou-Donia MB. 1996. P-glycoprotein involvement in cuticular penetration of [¹⁴C]thiodicarb in resistant tobacco budworms. Toxicol Lett 85:127–133.
17. Hou W, Jiang C, Zhou X, Qian K, Wang L, Shen Y, Zhao Y. 2016. Increased expression of P-glycoprotein is associated with chlorpyrifos resistance in the German cockroach (Blattodea: Blattellidae). J Econ Entomol 109:2500–2505.
18. Luo L, Sun YJ, Wu YJ. 2013. Abamectin resistance in *Drosophila* is related to increased expression of P-glycoprotein via the dEGFR and dAkt pathways. Insect Biochem Mol Biol 43:627–634.
19. Tian L, Yang J, Hou W, Xu B, Xie W, Wang S, Zhang Y, Zhou X, Wu Q. 2013.

- 592 Molecular cloning and characterization of a P-glycoprotein from the
593 diamondback moth, *Plutella xylostella* (Lepidoptera: Plutellidae). Int J Mol Sci
594 14:22891–22905.
- 595 20. Fligel LE, Swarup S, Chen M, Bauer C, Wanjugi H, Carroll M, Hill P, Tuscan M,
596 Bansal R, Flannagan R, Clark TL, Michel AP, Head GP, Goldman BS. 2015.
597 Genetic markers for western corn rootworm resistance to Bt toxin. G3 5:399–
598 405.
- 599 21. Pauchet Y, Bretschneider A, Augustin S, Heckel DG. 2016. A P-glycoprotein is
600 linked to resistance to the *Bacillus thuringiensis* Cry3Aa toxin in a leaf beetle.
601 Toxins 8:362.
- 602 22. Niu X, Kassa A, Hasler J, Griffin S, Perez-Ortega C, Procyk L, Zhang J,
603 Kapka-Kitzman DM, Nelson ME, Lu A. 2020. Functional validation of
604 DvABCB1 as a receptor of Cry3 toxins in western corn rootworm, *Diabrotica*
605 *virgifera virgifera*. Sci Rep 10:15830.
- 606 23. Zhou J, Guo Z, Kang S, Qin J, Gong L, Sun D, Guo L, Zhu L, Bai Y, Zhang Z,
607 Zhou X, Zhang Y. 2020. Reduced expression of the P-glycoprotein gene
608 *PxABCB1* is linked to resistance to *Bacillus thuringiensis* Cry1Ac toxin in
609 *Plutella xylostella* (L.). Pest Manag Sci 76:712–720.
- 610 24. Guo Z, Kang S, Sun D, Gong L, Zhou J, Qin J, Guo L, Zhu L, Bai Y, Ye F, Wu Q,
611 Wang S, Crickmore N, Zhou X, Zhang Y. 2020. MAPK-dependent hormonal
612 signaling plasticity contributes to overcoming *Bacillus thuringiensis* toxin action
613 in an insect host. Nat Commun 11:3003.

- 614 25. Callaghan R, Crowley E, Potter S, Kerr ID. 2008. P-glycoprotein: so many ways
615 to turn it on. *J Clin Pharmacol* 48:365–378.
- 616 26. Katayama K, Noguchi K, Sugimoto Y. 2014. Regulations of
617 P-Glycoprotein/ABCB1/*MDR1* in human cancer cells. *New J Sci* 2014:1–10.
- 618 27. Guo Z, Kang S, Chen D, Wu Q, Wang S, Xie W, Zhu X, Baxter SW, Zhou X,
619 Jurat-Fuentes JL, Zhang Y. 2015. MAPK signaling pathway alters expression of
620 midgut ALP and ABCC genes and causes resistance to *Bacillus thuringiensis*
621 Cry1Ac toxin in diamondback moth. *PLoS Genet* 11:e1005124.
- 622 28. Guo Z, Sun D, Kang S, Zhou J, Gong L, Qin J, Guo L, Zhu L, Bai Y, Luo L,
623 Zhang Y. 2019. CRISPR/Cas9-mediated knockout of both the *PxABCC2* and
624 *PxABCC3* genes confers high-level resistance to *Bacillus thuringiensis* Cry1Ac
625 toxin in the diamondback moth, *Plutella xylostella* (L.). *Insect Biochem Mol*
626 *Biol* 107:31–38.
- 627 29. Guo Z, Qin J, Zhou X, Zhang Y. 2018. Insect transcription factors: a landscape of
628 their structures and biological functions in *Drosophila* and beyond. *Int J Mol Sci*
629 19:3691.
- 630 30. Li J, Ma Y, Yuan W, Xiao Y, Liu C, Wang J, Peng J, Peng R, Soberón M, Bravo
631 A, Yang Y, Liu K. 2017. FOXA transcriptional factor modulates insect
632 susceptibility to *Bacillus thuringiensis* Cry1Ac toxin by regulating the
633 expression of toxin-receptor *ABCC2* and *ABCC3* genes. *Insect Biochem Mol*
634 *Biol* 88:1–11.
- 635 31. Wei W, Pan S, Ma Y, Xiao Y, Yang Y, He S, Bravo A, Soberón M, Liu K. 2020.

- 636 GATAe transcription factor is involved in *Bacillus thuringiensis* Cry1Ac toxin
637 receptor gene expression inducing toxin susceptibility. Insect Biochem Mol Biol
638 118:103306.
- 639 32. Yang X, Deng S, Wei X, Yang J, Zhao Q, Yin C, Du T, Guo Z, Xia J, Yang Z, Xie
640 W, Wang S, Wu Q, Yang F, Zhou X, Nauen R, Bass C, Zhang Y. 2020.
641 MAPK-directed activation of the whitefly transcription factor *CREB* leads to
642 P450-mediated imidacloprid resistance. Proc Natl Acad Sci U S A 117:10246–
643 10253.
- 644 33. Zabidi MA, Stark A. 2016. Regulatory enhancer-core-promoter communication
645 via transcription factors and cofactors. Trends Genet 32:801–814.
- 646 34. Ye N, Ding Y, Wild C, Shen Q, Zhou J. 2014. Small molecule inhibitors targeting
647 activator protein 1 (AP-1). J Med Chem 57:6930–6948.
- 648 35. Atsaves V, Leventaki V, Rassidakis GZ, Claret FX. 2019. AP-1 transcription
649 factors as regulators of immune responses in cancer. Cancers 11:1037.
- 650 36. Kockel L, Homsy JG, Bohmann D. 2001. *Drosophila* AP-1: lessons from an
651 invertebrate. Oncogene 20:2347–2364.
- 652 37. Sanyal S, Sandstrom DJ, Hoeffler CA, Ramaswami M. 2002. AP-1 functions
653 upstream of CREB to control synaptic plasticity in *Drosophila*. Nature 416:870–
654 874.
- 655 38. Wray GA. 2007. The evolutionary significance of *cis*-regulatory mutations. Nat
656 Rev Genet 8:206–216.
- 657 39. Shaulian E, Karin M. 2002. AP-1 as a regulator of cell life and death. Nat Cell

- 658 Biol 4:E131–E136.
- 659 40. McNeill MS, Robinson GE. 2015. Voxel-based analysis of the immediate early
660 gene, *c-jun*, in the honey bee brain after a sucrose stimulus. *Insect Mol Biol*
661 24:377–390.
- 662 41. Tafesh-Edwards G, Eleftherianos I. 2020. JNK signaling in *Drosophila* immunity
663 and homeostasis. *Immunol Lett* 226:7–11.
- 664 42. Chen Q, Bian Y, Zeng S. 2014. Involvement of AP-1 and NF- κ B in the
665 up-regulation of P-gp in vinblastine resistant Caco-2 cells. *Drug Metab*
666 *Pharmacokinet* 29:223–226.
- 667 43. Miao ZH, Ding J. 2003. Transcription factor c-Jun activation represses *mdr-1*
668 gene expression. *Cancer Res* 63:4527–4532.
- 669 44. Zhou J, Liu M, Aneja R, Chandra R, Lage H, Joshi HC. 2006. Reversal of
670 P-glycoprotein-mediated multidrug resistance in cancer cells by the c-Jun
671 NH2-terminal kinase. *Cancer Res* 66:445–452.
- 672 45. Tang PM, Zhang DM, Xuan NH, Tsui SK, Waye MM, Kong SK, Fong WP, Fung
673 KP. 2009. Photodynamic therapy inhibits P-glycoprotein mediated multidrug
674 resistance via JNK activation in human hepatocellular carcinoma using the
675 photosensitizer pheophorbide a. *Mol Cancer* 8:56.
- 676 46. Zhang K, Chaillet JR, Perkins LA, Halazonetis TD, Perrimon N. 1990.
677 *Drosophila* homolog of the mammalian jun oncogene is expressed during
678 embryonic development and activates transcription in mammalian cells. *Proc*
679 *Natl Acad Sci U S A* 87:6281–6285.

- 680 47. Bhaskara S, Chandrasekharan MB, Ganguly R. 2008. Caffeine induction of
681 *Cyp6a2* and *Cyp6a8* genes of *Drosophila melanogaster* is modulated by cAMP
682 and D-JUN protein levels. *Gene* 415:49–59.
- 683 48. Dunn C, Wiltshire C, MacLaren A, Gillespie DA. 2002. Molecular mechanism
684 and biological functions of c-Jun N-terminal kinase signalling via the c-Jun
685 transcription factor. *Cell Signal* 14:585–593.
- 686 49. Chiarini F, Del Sole M, Mongiorgi S, Gaboardi GC, Cappellini A, Mantovani I,
687 Follo MY, McCubrey JA, Martelli AM. 2008. The novel Akt inhibitor, perifosine,
688 induces caspase-dependent apoptosis and downregulates P-glycoprotein
689 expression in multidrug-resistant human T-acute leukemia cells by a
690 JNK-dependent mechanism. *Leukemia* 22:1106–1116.
- 691 50. Zhu X, Lei Y, Yang Y, Baxter SW, Li J, Wu Q, Wang S, Xie W, Guo Z, Fu W,
692 Zhang Y. 2015. Construction and characterisation of near-isogenic *Plutella*
693 *xylostella* (Lepidoptera: Plutellidae) strains resistant to Cry1Ac toxin. *Pest*
694 *Manag Sci* 71:225–233.
- 695 51. Guo Z, Kang S, Zhu X, Wu Q, Wang S, Xie W, Zhang Y. 2015. The midgut
696 cadherin-like gene is not associated with resistance to *Bacillus thuringiensis*
697 toxin Cry1Ac in *Plutella xylostella* (L.). *J Invertebr Pathol* 126:21–30.
- 698 52. Guo Z, Gong L, Kang S, Zhou J, Sun D, Qin J, Guo L, Zhu L, Bai Y, Bravo A,
699 Soberón M, Zhang Y. 2020. Comprehensive analysis of Cry1Ac protoxin
700 activation mediated by midgut proteases in susceptible and resistant *Plutella*
701 *xylostella* (L.). *Pestic Biochem Physiol* 163:23–30.

- 702 53. Xie W, Lei Y, Fu W, Yang Z, Zhu X, Guo Z, Wu Q, Wang S, Xu B, Zhou X,
703 Zhang Y. 2012. Tissue-specific transcriptome profiling of *Plutella xylostella* third
704 instar larval midgut. *Int J Biol Sci* 8:1142–1155.
- 705 54. Guo Z, Kang S, Zhu X, Xia J, Wu Q, Wang S, Xie W, Zhang Y. 2015. The novel
706 ABC transporter ABCH1 is a potential target for RNAi-based insect pest control
707 and resistance management. *Sci Rep* 5:13728.

708 **Figure Legends**

709 **Figure 1.** Transcriptional activity of the *PxABCB1* promoter in susceptible and
710 resistant *P. xylostella*. (A) A diagram of sequence alignment of the 5'-flanking
711 regions of *PxABCB1* in the susceptible DBM1Ac-S and resistant NIL-R strains. The
712 right-angled arrow denotes the TSS. The numbers with arrows specify the 5' and 3'
713 positions of the corresponding nucleotide. The green/white rectangles indicate DNA
714 fragment insertion/deletion (Ins/Del). (B) Detection of *PxABCB1* promoter activities
715 in susceptible and resistant *P. xylostella*. All the fragment constructs are named with
716 "P" as the starting letter, followed by a pair of parentheses that contain two
717 numerals, separated by a dash (/), to specify the 5' and 3' positions of the
718 corresponding promoter fragment. Relative luciferase (*Luc*) activities were detected
719 at 48 h post-transfection in S2 cells. The relative luciferase activity (fold) of different
720 promoter recombinants was calculated based on the value of the pGL4.10 control
721 vector. The values shown are the means and the corresponding standard error (SEM)
722 for three independent experiments. The significance of differences was determined
723 by one-way ANOVA with Duncan's test ($p < 0.05$).

724

725 **Figure 2.** Relative luciferase activity analysis of the fragments between -765 and
726 +125. Progressive 5' deletion constructs from -765 to +125 were transfected into S2
727 cells, and luciferase activity was detected. The relative luciferase activity (fold) of
728 different constructs was calculated based on the value of the pGL4.10 vector. The
729 values shown are the means and the corresponding standard error (SEM). One-way

ANOVA followed by Duncan's test was used for comparison ($p < 0.05$, $n = 3$).

731

732 **Figure 3.** Effects of potential transcription factors (TFs) on the activity of the
733 *PxABCB1* promoter. (A) Putative transcription factor binding sites (TFBSs) in
734 critical positive and negative regulatory regions (see Fig. S1 for detailed DNA
735 motifs). Different colored ellipses represent different TFBSs. (B) Effects of different
736 predicted TFs on *PxABCB1* promoter activity. Every cloned TF was subcloned into
737 the pAc5.1 expression vector to generate a recombinant vector, which was then
738 co-transfected with P(-1122/+125) to determine the luciferase activity. The empty
739 pAc5.1 without PxJun was used as a control. The relative luciferase activity (fold)
740 was calculated based on the value of the empty pAc5.1 vector. The values shown are
741 the means and the corresponding standard error (SEM). One-way ANOVA followed
742 by Duncan's test was used for statistical analysis ($p < 0.05$, $n = 3$).

743

744 **Figure 4.** PxJun represses *PxABCB1* promoter activity through the Jun binding site
745 (JBS). (A) Effect of PxJun on *PxABCB1* promoter activity with either a deleted or a
746 mutated form of the JBS via the dual-luciferase reporter assay. The JBS motif
747 (AAGAAATGAGAGAT, -107 to -94) in P(-1122/+125) was deleted or mutated to
748 GGAGGGCAGAGAGC. PxJun was co-transfected with P(-1122/+125) containing
749 normal JBS (red ellipse), deleted JBS (black ellipse) or mutated JBS (green ellipse).
750 The empty pAc5.1 without PxJun was used as a control. Three biological replicates
751 were performed for all experiments. The values shown are the means and the
752 corresponding standard error (SEM). One-way ANOVA followed by Duncan's test

753 was used for statistical analysis ($p < 0.05$). (B) Verification of direct binding of
754 PxJun to the JBS by the yeast one-hybrid assay (Y1H). Three tandem repeats
755 containing wild-type or mutated JBS sequences were fused to the pABAI vector,
756 which was subsequently integrated into the Y1HGold yeast strain to generate the
757 “bait strain”. A critical aureobasidin A (AbA) concentration of 500 ng/mL was
758 detected to completely repress the growth of the bait strains on SD/-Ura media.
759 PxJun was fused to the pGATD7 vector and then transferred into the “bait strain”,
760 which was grown on SD/-Leu selective media with or without AbA. EV, empty
761 vector; positive control, using pGADT7-p53 + pABAI-p53.

762

763 **Figure 5.** Effects of PxJun and/or PxFos on the activity of the *PxABCB1* promoter.
764 PxJun and/or PxFos were co-transfected with P(-1122/+125), and the luciferase
765 activity was measured. The empty pAc5.1 without TF was used as a control. The
766 relative luciferase activity (fold) was calculated based on the value of the empty
767 pAc5.1 vector. The values shown are the means and the corresponding standard error
768 (SEM) for three independent experiments. One-way ANOVA followed by Duncan’s
769 test was used for statistical analysis ($p < 0.05$, $n = 3$).

770

771 **Figure 6.** The relative expression levels of the *PxJun* gene in the midgut tissues of
772 fourth-instar larvae in five *P. xylostella* strains as detected by qPCR. The *RPL32*
773 gene was used as an internal control. The relative expression level (fold) is presented
774 as the ratio to the value of the lowest expression level, observed in the DBM1Ac-S

775 strain. The average relative expression level and SEM of three independent
776 replicates are presented. Different letters used to mark bars denote significant
777 differences ($p < 0.05$, Duncan's test, $n = 3$).

778

779 **Figure 7.** Effect of *PxJun* gene silencing on *PxABCB1* expression and Cry1Ac
780 resistance in resistant NIL-R larvae. (A) Relative expression of *PxJun* and *PxABCB1*
781 at 48 h post-injection with buffer, dsEGFP or dsPxJun. The expression levels of
782 *PxJun* or *PxABCB1* in the control larvae injected with buffer were set as 1. (B)
783 Silencing of *PxJun* expression decreased the resistance of NIL-R larvae to Cry1Ac
784 protoxin. At 48 h after microinjection with buffer, dsEGFP or dsPxJun, the larvae
785 were fed diets with or without Cry1Ac protoxin (1000 mg/L). The percentage of
786 larval mortality was then counted at 72 h post-treatment. Data are presented as the
787 mean values \pm SEM for three biologically independent experiments. Different letters
788 in each group indicate statistically significant differences between treatments ($P <$
789 0.05 ; Duncan's test; $n = 3$).

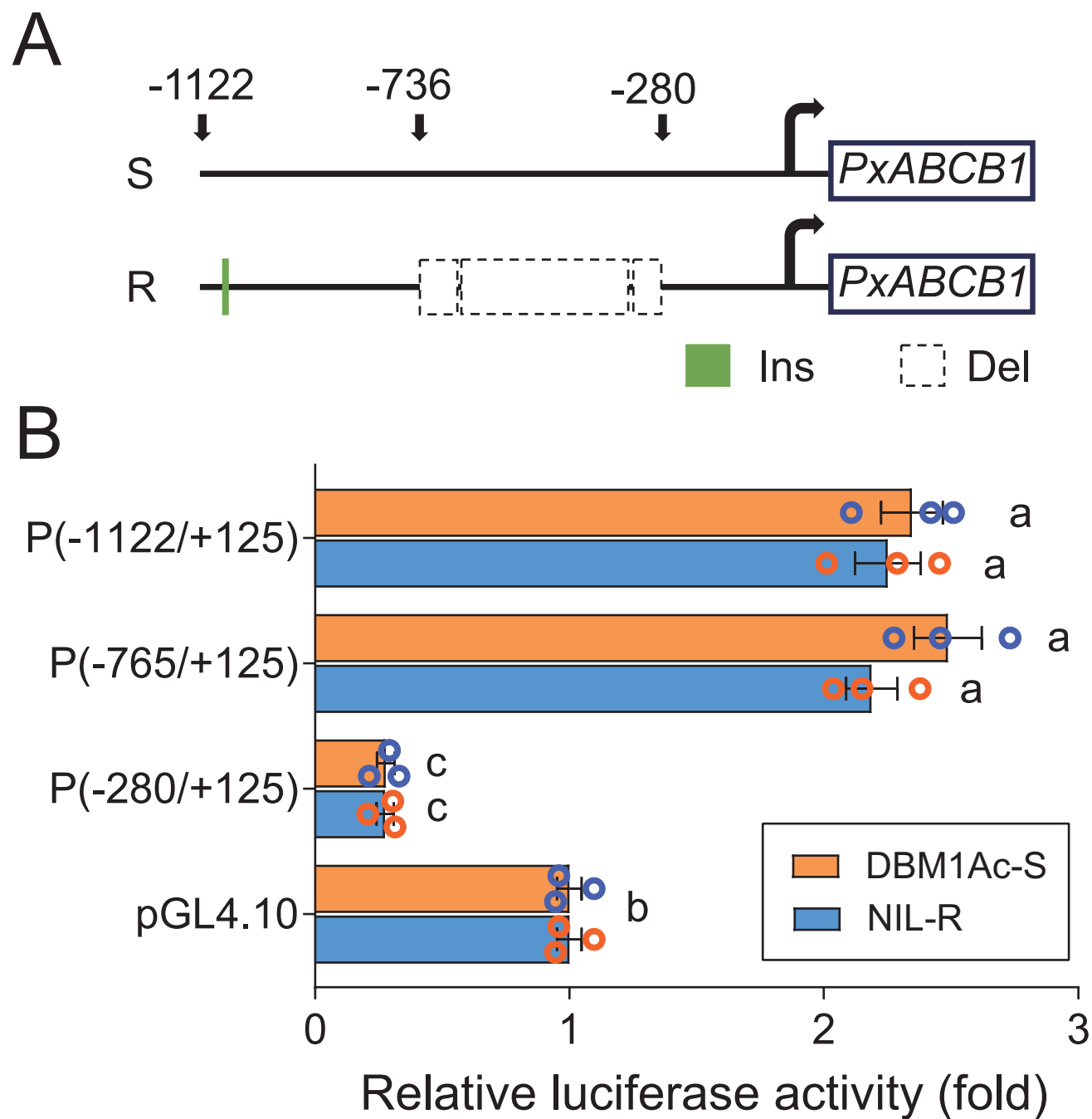
790

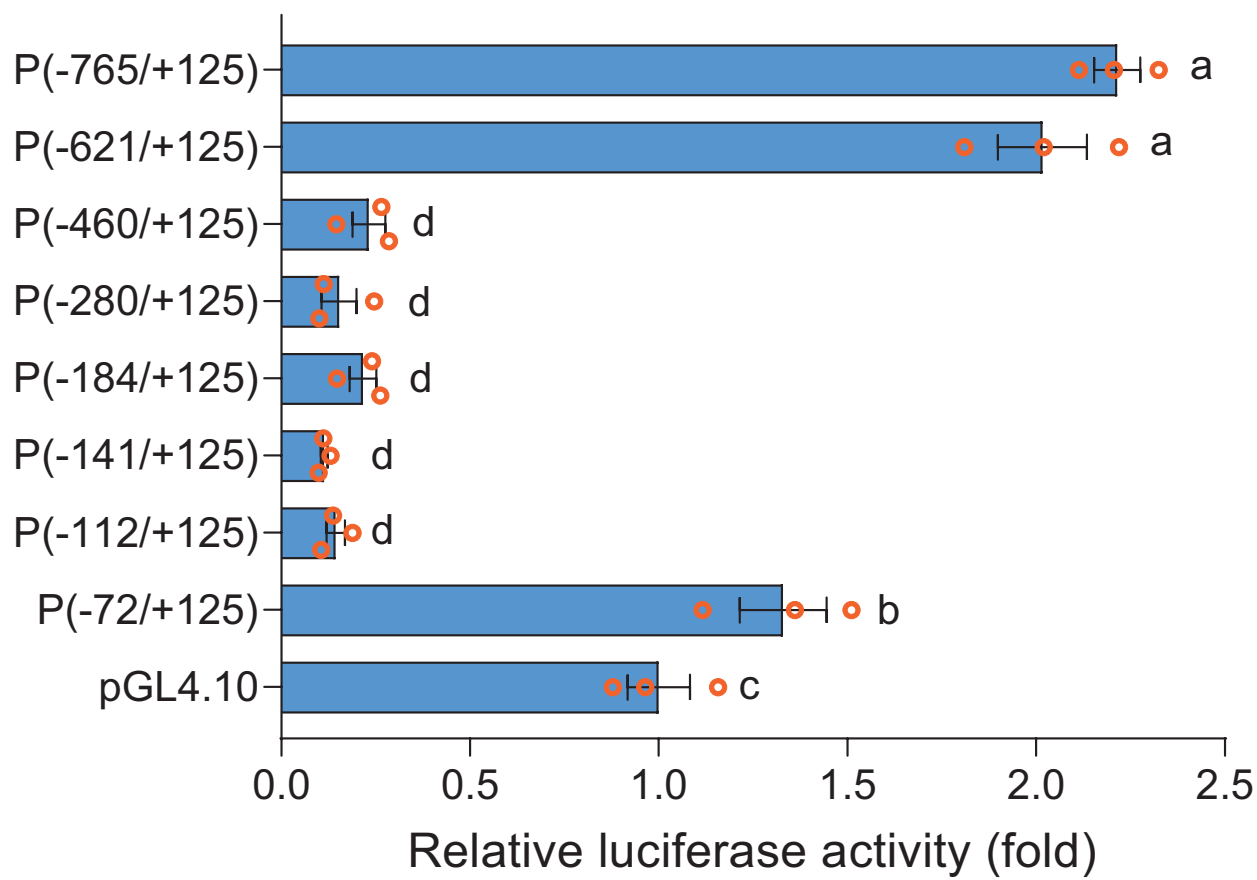
791 **Figure 8.** Effect of *PxMAP4K4* gene silencing on the expression levels of *PxJun* and
792 *PxABCB1* in the midgut tissues at different periods. Data are presented as the mean
793 values \pm SEM for three biologically independent experiments. Asterisks (*) indicate
794 significant differences among periods for each gene ($P < 0.05$; Duncan's test; $n = 3$).

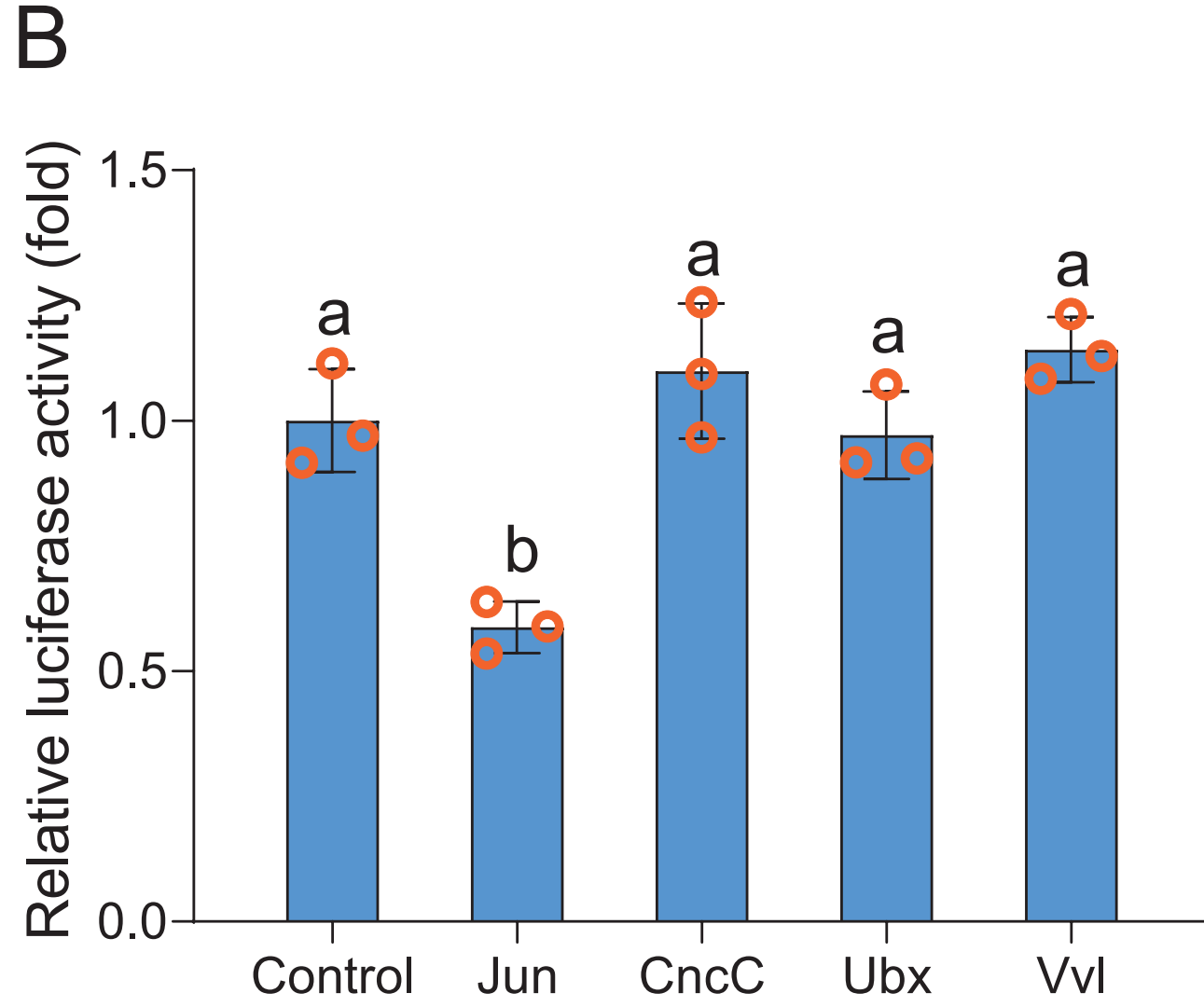
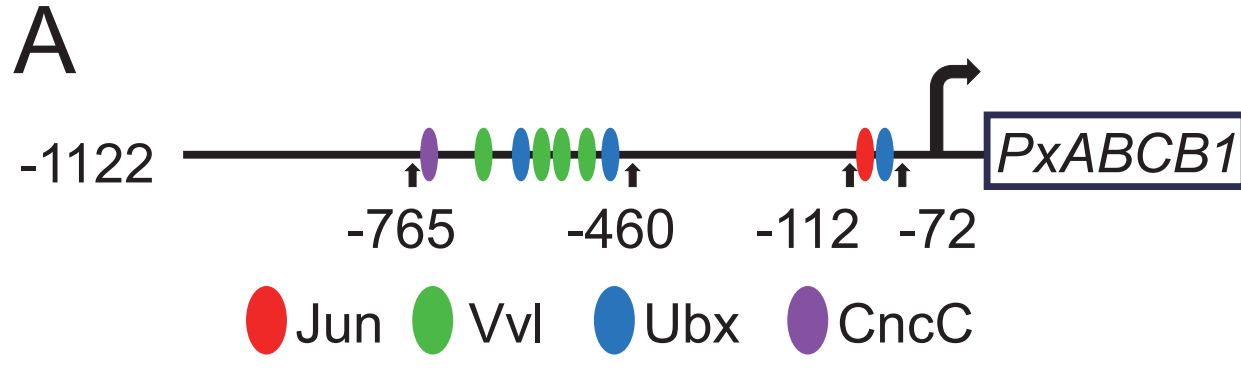
795

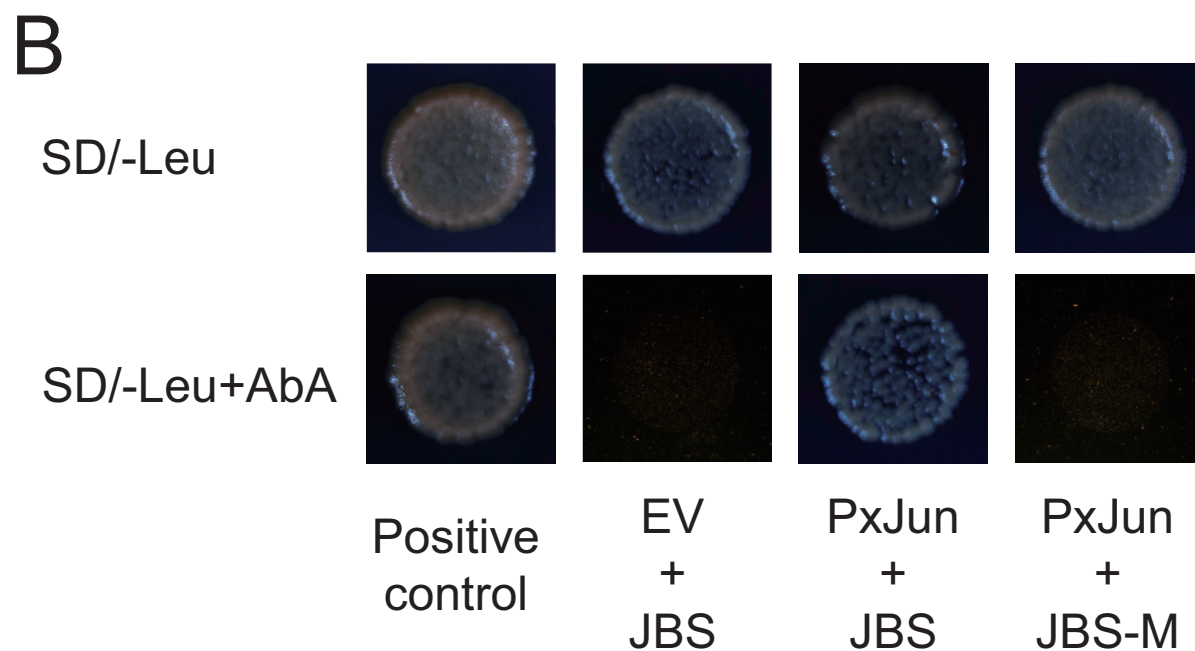
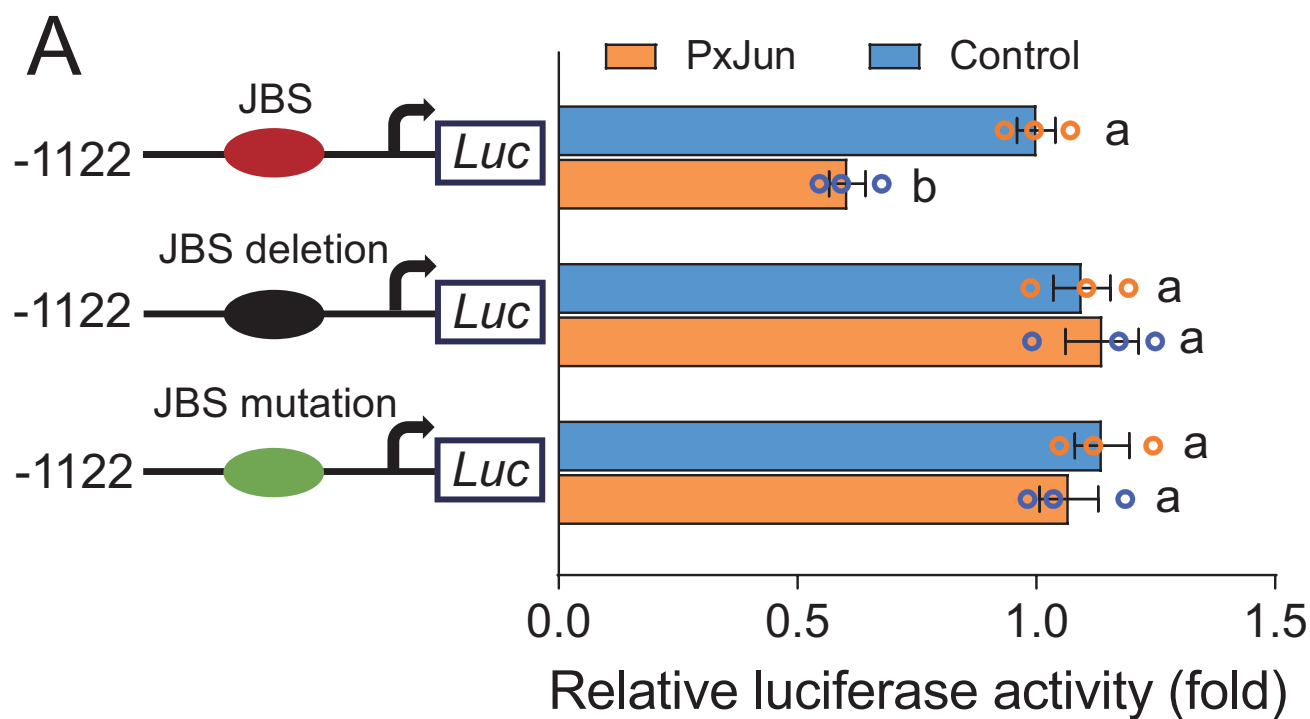
796 **Figure 9.** A proposed model for the transcriptional regulation of reduced *PxABCB1*
797 expression by the MAPK-activated TF PxJun. The activated MAPK signaling

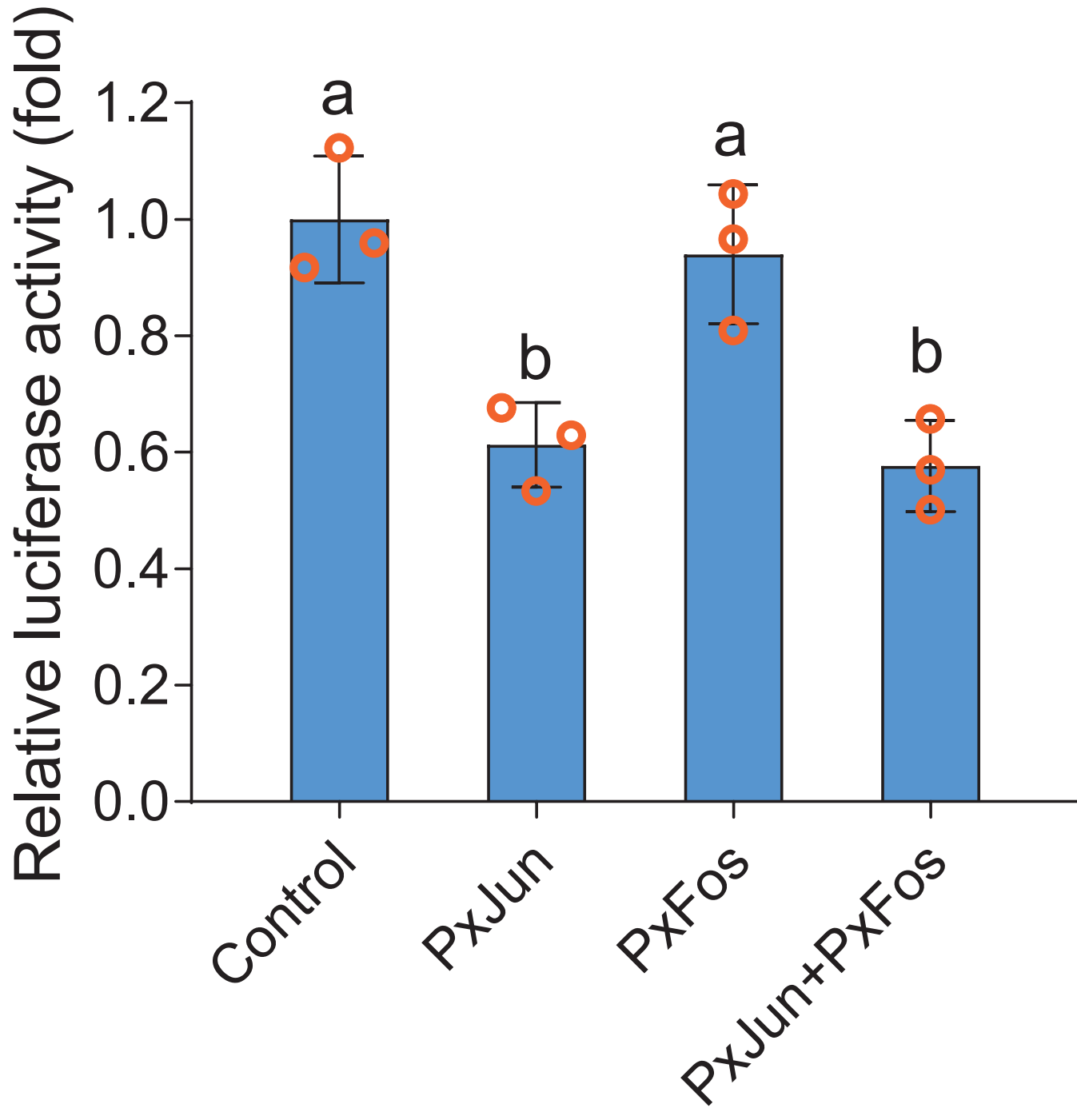
798 pathway increases the expression of *PxJun*, which in turn represses the transcript
799 level of Bt Cry1Ac receptor gene *PxABCBI* and enhances larval resistance to Bt
800 Cry1Ac toxin in *P. xylostella*.

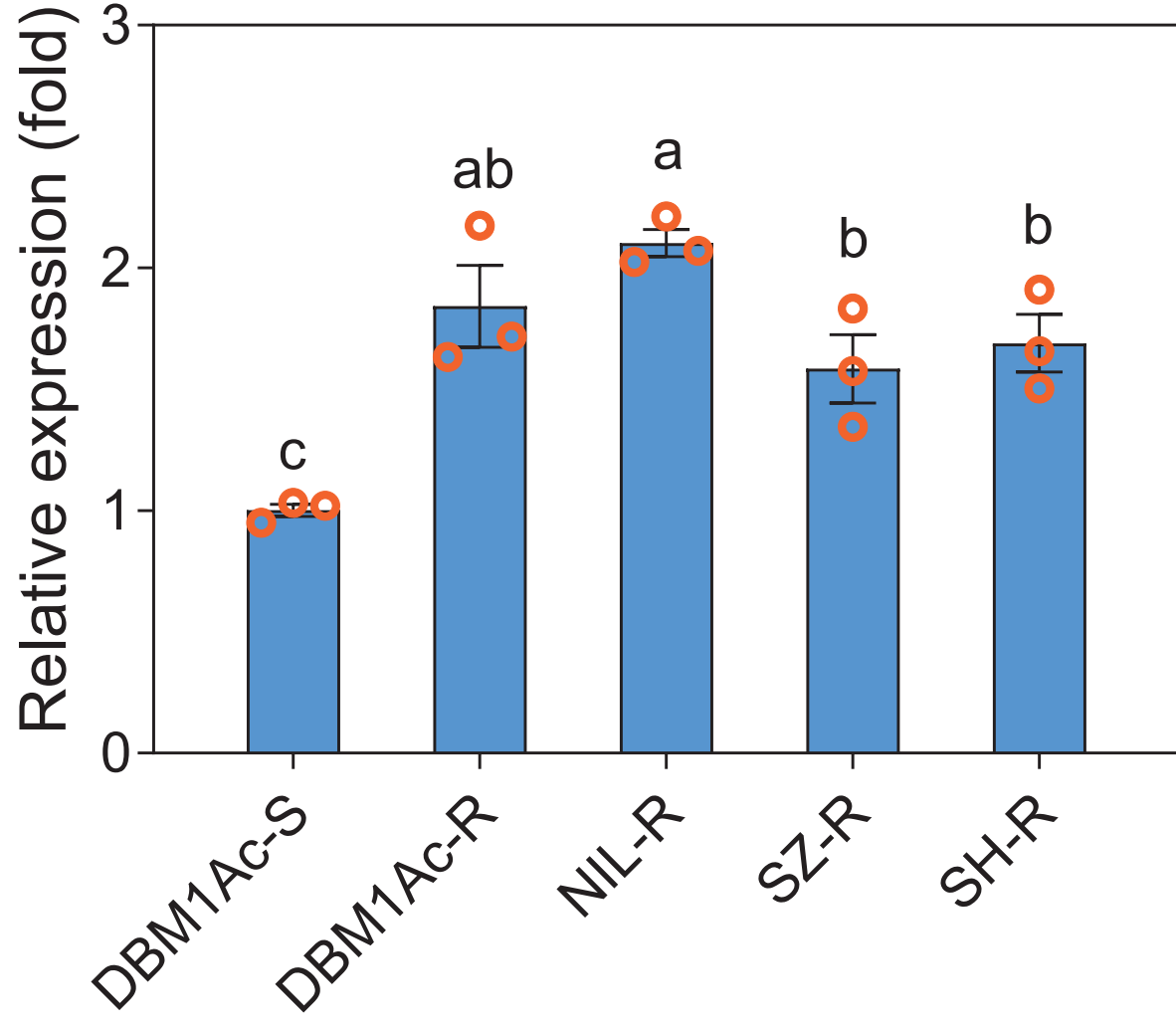


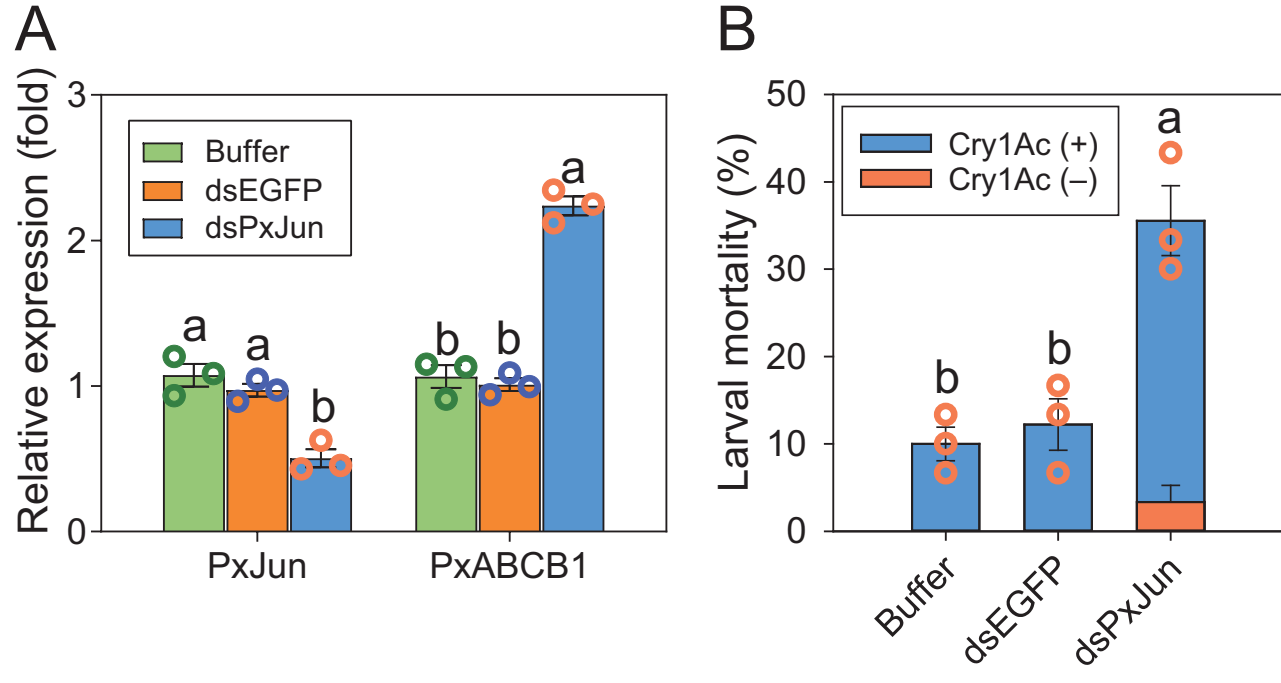


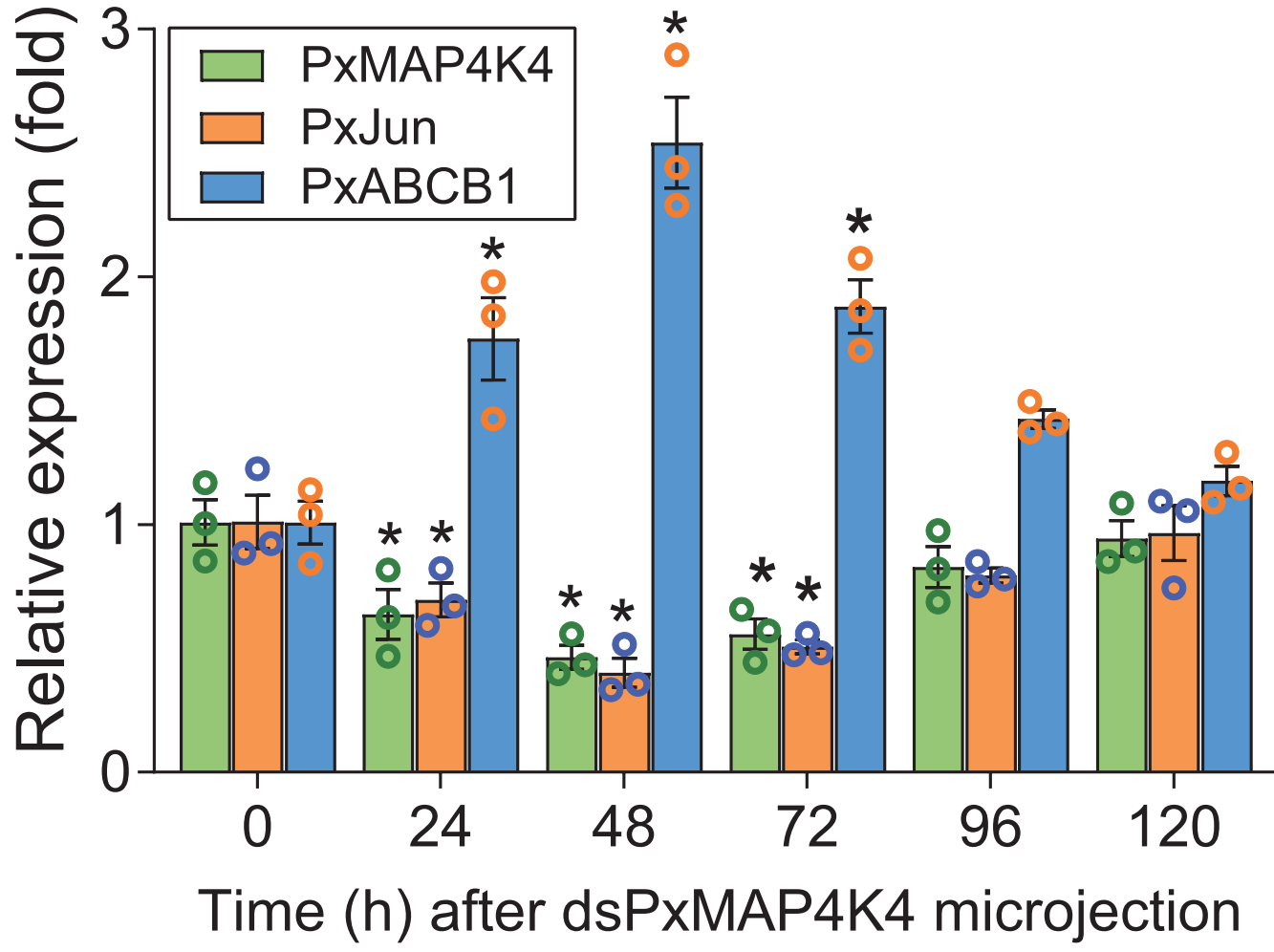




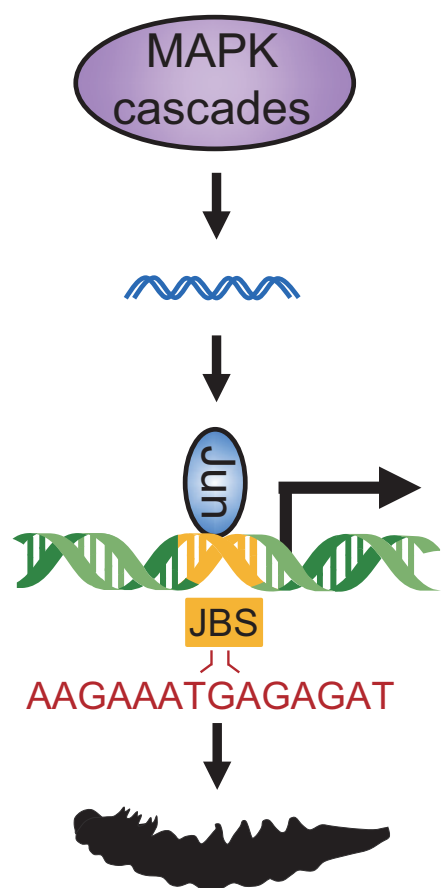








Bt susceptible *P. xylostella*



Bt resistant *P. xylostella*

